Maskless production of neural-recording graphene microelectrode arrays

Vanessa Pereira Gomes,[1,a)] Aline Maria Pascon,[2] Roberto Ricardo Panepucci,[3] and Jacobus Willibrordus Swart[4]
[1]*School of Electrical and Computer Engineering, State University of Campinas, 400 Albert Einstein Avenue, Campinas, São Paulo 13083852, Brazil*
[2]*Center of Semiconductor Components and Nanotechnologies, State University of Campinas, 90 João Pandiá Calógeras Street, Campinas, São Paulo 13083870, Brazil*
[3]*Center of Information Technology Renato Archer, Dom Pedro I Highway (SP-65), Km 143.6, Amarais, Campinas, São Paulo 13069901, Brazil*
[4]*Semiconductor, Instruments and Photonics Department, State University of Campinas, 400 Albert Einstein Avenue, Campinas, São Paulo 13083852, Brazil*

(Received 11 July 2018; accepted 16 January 2019; published 1 February 2019)

This paper describes the production of a new version of high-performance microelectrode arrays (MEAs) that can be custom produced and used to explore *in vitro* neural networks. The MEAs were manufactured using direct write technology and comprised graphene microelectrodes and SU-8 insulation on a glass substrate, where graphene was grown by chemical vapor deposition on copper foil and then transferred to the substrate. The graphene MEAs experimentally exhibited adequate electrical specifications, with the electrode characterized using noise testing, cyclic voltammetry, and impedance spectroscopy. The MEAs herein exhibited improved properties over those previously reported in the literature. The average impedance at 1 kHz for the electrodes herein was 5.2 kΩ, which is compatible with commercial MEAs which present values between 30 and 400 kΩ. Further, the MEA device herein did not show biotoxicity and is thus adequate for cellular potential measurements. *Published by the AVS.* https://doi.org/10.1116/1.5048216

I. INTRODUCTION

Neurons are the essential elements for the transmission of information in the body. Neurons can connect to thousands of different cells, and these connections are responsible for producing the signals that enable a person to walk and breathe and recall a fact, for example. Based on this, several researchers have focused their studies on the normal functioning of neural networks and why they stop working properly in a patient suffering from a disease. Furthermore, it is essential to study the electrophysiology of single neurons and the structural and functional relationship of neural networks, which both modulate cognitive functions and are vital for generating treatments for neurological and psychiatric disorders.[1,2]

In this scenario, an interesting option for neural study is microelectrode arrays (MEAs), as represented in Fig. 1, which is an instrument specially designed to study electrically excitable cells. The MEA consists of a set of microelectrodes employed to measure the action potentials of neurons and/or muscle cells.[3]

The advantages of the MEA are threefold and include (1) the ability to record the electrophysiological activity of cells for long periods of time (up to weeks) without damaging them, as well as to stimulate and image the cells during the experiment; (2) the ability to noninvasively investigate the interactions between cells at different positions in the same tissue; and (3) the fact that the MEA can be used as a neuroimplant, which is a long-term prosthetic device capable of controlling and/or replacing the function of a tissue in an injured nervous system.[4–6] Some MEA applications include the ability to highlight the spontaneous activity of a neural network and its response to applied electrical or chemical stimuli, its plasticity, and for drug monitoring.[4,7] In neuroscience applications, previous works have reported electrical measurement of brain tissue slices,[8] dissociated neuronal cultures,[9] retinas,[10] and cardiomyocytes.[11] These applications are possible because neuronal cell cultures deposited on the MEA quickly adhere to its surface and connect directly with the microelectrodes. When excited, the neurons and muscle cells generate an extracellular ionic current through their membranes and generate a change in voltage at this region. This event triggers an extracellular voltage at the electrode that is detected. During stimulation, the MEA microelectrodes convert an electronic current into an ionic current through the medium, which affects the voltage-dependent ion channels (such as sodium and potassium channels). This promotes cell depolarization and, consequently, triggers neuronal action potentials or muscle cell contractions.[6] Further, MEAs have the ability to record the propagation of signals from neural networks without causing damage to them because the main receptor and synaptic and cellular mechanisms that produce the activity patterns are preserved. This is not true of traditional invasive methods, such as the patch clamp, which can cause damage to the neural networks.[3]

A standard MEA consists of an array of 8×8 microelectrodes (interelectrode distance of 100–200 μm) in the central region, placed under a transparent insulation layer and a sample-containment ring.[4,6,7] The device itself can be divided into five parts: substrate, interlayer, conductor, insulation, and ring. The substrate supports all of the MEA device layers. The main issue for substrate material choice is

a)Electronic mail: pgomes.vanessa@gmail.com

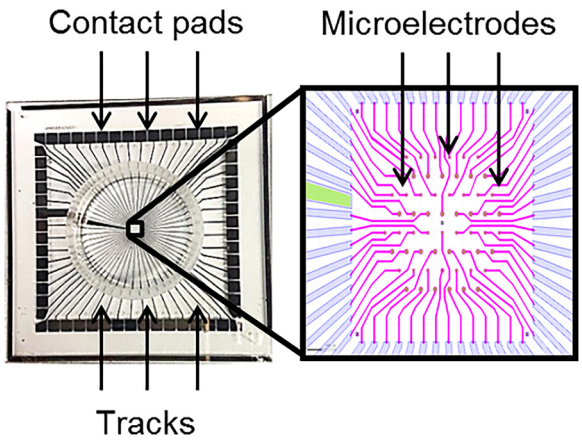

FIG. 1. Photograph (left) and layout of the microelectrodes (right) of the fabricated MEA. Circular electrodes are located in the central region. Tracks and contact pads conduct the signal registered by the electrodes to the measurement setup. The edge of the square pad frame is 4.9 mm.

its transparency because inverted microscopy is used to monitor cell culture analysis in liquid deposited on the MEA. There is a wide range of substrate material possibilities such as sapphire, silicon, parylene, and glass, where the latter exhibits the qualities of good transparency, chemical resistance, thermal stability, electrical insulation (minimizing parasitic elements usually found in silicon), relatively low cost compared to silicon, and other options, eliminates the need for an insulation layer between itself and the conduction layer, and biocompatibility.[4,12] The next step in the MEA manufacture is the interlayer, which basically comprises an insulating layer between the substrate and the conductor and is intended to prevent the migration of substrate contaminants to the subsequent layers and to improve the adhesion of the conductor to the substrate. Although including the interlayer is not a mandatory practice for traditional MEA platforms, its adoption is quite interesting because certain substrates are not insulating, such as silicon. Most common interlayer materials include silicon dioxide (SiO_2), silicon nitride (Si_3N_4), and amorphous silicon (α-Si), and the interlayer thickness can be up to 100 nm.[13]

The next MEA layer is related to signal conduction and comprises the electrodes, tracks, and contact pads, with typical thickness between 60 and 445 nm.[6] The conductor material must exhibit a good long-term performance, high charge injection capacity (CIC), low impedance (below 1 MΩ at 1 kHz, which is the standard reference level for neural impedance analysis), and biocompatibility.[14,15] These material attributes minimize thermal noise and enable the measurement of small extracellular neural signals (10–100 μV) and the transmission of a stimulation current through the microelectrodes without exceeding the electrolysis window of water and other components of the medium (~1 V).[16] Typically, titanium nitride (TiN) is used as the electrode material[16] owing to its stability, biocompatibility, low impedance, high degree of hardness (higher than black platinum), high wear and corrosion resistance, and high CIC.[9] In addition, graphene has been gaining prominence as an MEA conductor for several applications because it combines the interesting features of flexibility and low noise to its other features of excellent electrical and thermal conductivity, mechanical and electrochemical stability, transferability, high mechanical strength (greater than 0.5 TPa), good CIC, and broad-spectrum transparency. There have been reports of electrodes covered with graphene and incubated for weeks with neuronal primary cells, which then exhibit good cell adhesion and good biocompatibility and can detect neural signals with high resolution *in vivo*.[1,2,16,17]

The next MEA layer is the insulation, which covers the entire MEA except the electrodes and contact pads. The insulating layer is essential to the proper functioning of this device because it prevents parasitic capacitances and conductivity between the electrodes and the culture medium. In addition, the insulation material must be inert to prevent degradation because MEAs are used for experiments that employ solutions with large amounts of ions.[4,6] The typical insulation materials are SiO_2 (Ref. 6) and Si_3N_4 (Ref. 7) in a layer up to 1 μm thick. However, this thinness of an insulation layer may be unable to reduce parasitic capacitances. An alternative material is a polymer such as SU-8, which is transparent, can be deposited in thickness on the order of several micrometers, has high chemical stability, and does not induce any toxic effect in cells.[4,13]

The final MEA component is the ring, whose main purpose is to create a reservoir to contain the biological materials. The rings are typically made of Teflon or glass and are sealed with biocompatible glue to ensure that the contents remain in the active area of the MEA platform.[7]

Herein, we propose a new manufacturing method for graphene-based MEAs, including the MEA design and the description of all the manufacturing steps, the materials, the procedures, and the characterization of the final product. Further, we perform experimental analysis of the fabricated graphene-based MEAs to characterize their electrical specifications and compare them to standard commercial MEAs.

II. EXPERIMENT

Herein, we produce an array comprising graphene microelectrodes that is entirely manufactured through direct writing, without the need for photomask production. We developed a direct laser writing process. We aligned exposures with a direct write system (Heidelberg DWL66FS, Heidelberg, Germany) using a 405 nm laser for the MEA conductive region, as well as using modified SU-8 with a photoinitiator active at the 405 nm exposure. Further, the system was equipped with a high-resolution pattern generator capable of creating patterns and directing an exposure on the wafer in the scale of micrometers and submicrometers without the requirement of lithographic photomasks.

The design of the MEA layout herein consisted of a set of 60 circular microelectrodes with diameters of 20 and 40 μm distributed in an octagonal format. In general, the electrode diameter can range from 5 to 160 μm, depending on the application.[4,13] Considering that the diameter of the dorsal root ganglion neuron of Wistar rats is between 15 and 40 μm,[18] the microelectrode dimensions of 20 and 40 μm chosen here are

adequate to detect electrical signals from these cell cultures. In addition, neurons in brain slices have signal sources within a 30 μm radius around the center of the microelectrode and can be detected at a distance up to 100 μm, which is the range of our microelectrode. Using this mask design, the manufacturing process of the MEAs was based on the conventional microfabrication method used with silicon, as adapted for the glass substrate. Sections II A–II E discuss the aspects related to the manufacture of the MEA herein for each layer: (A) substrate, (B) interlayer, (C) conductor, (D) insulation, and (E) ring.

A. Substrate

Because of the particular requirements required for MEA substrates discussed in Sec. I, glass was chosen for the substrate material. First, to remove any impurities from the substrate, the glass was cleaned by immersing it in a detergent solution (EXTRAN MA02 3% v/v, Merk) followed by rinsing with a deionized (DI) water flow for 1 min. Next, the glass substrate was dipped for 15 min in DI water, hydrogen peroxide (30%, Ultrapure Solutions Inc.), and ammonium hydroxide (29%, JT Baker) solution mixed at a ratio of 5:1:1.

B. Interlayer

After substrate cleaning, a 100 nm-thick transparent insulating layer of SiO_2 was deposited as the interlayer on the glass substrate using plasma-enhanced chemical vapor deposition (CVD, Oxford NGP-80, Abingdon, England).

C. Conductor

Next, the microelectrodes, tracks, and contact pads were fabricated on the interlayer by transferring the MEA pattern, thus defining the conductive region of the MEA device. Herein, we used TiN and graphene for the conductive materials. The microelectrodes were created using graphene on TiN, while tracks and contact pads were fabricated using only opaque TiN (see Fig. 1). Therefore, we note that most of the central area of our MEA is transparent, which facilitated the observation of the culture medium during cellular experiments.

First, the TiN tracks and contact pads were defined using the liftoff technique. First, a layer of AZ1518 (Microchem, Westborough, USA) photoresist was spun coated at 6000 rpm for 30 s and baked at 95 °C for 60 s on the SiO_2 interlayer. Second, the negative pattern of the tracks and contact pads was exposed via the direct laser writing process with the DWL66FS system, followed by standard immersion development in AZ726MIF for 60 s (Microchem, Westborough, USA), revealing the desired pattern. Then, a 100 nm layer of TiN was deposited on the sample with a ULVAC MHC-9000 reactive sputtering system using a Ti target and a 60:10 sccm flow of Ar:N_2 at 0.3 mTorr and 1 kW RF power at 13.56 MHz. Liftoff was subsequently performed in acetone to remove the photoresist and TiN over the resist in the unpatterned areas, thus forming the desired conductive regions on the MEA.[1]

Graphene was grown using a CVD process described elsewhere,[19] on both sides of a copper foil. The graphene was then transferred to the MEA via a modified wet transfer method using polymethyl methacrylate (PMMA) as the supporting layer.[20] For this method, after CVD growth of graphene on the Cu, PMMA was deposited on the graphene on one side of the Cu foil, followed by curing at 170 °C. Then, the graphene/Cu/graphene/PMMA stack was suspended in a 1:3 (HNO_3):(H_2O) solution to remove the unprotected graphene layer, followed by immersion in a Marble solution [$CuSO_4$ (620 mmol/l) with H_2O/HCl, 1:1] to remove the Cu foil. The resulting graphene/PMMA sample was washed in DI water and manually transferred to the desired region of MEA. The modifying step from Li *at al.*,[21] which was applied in the fabrication process of our MEAs, adds a second PMMA deposition by spin-coating to improve the contact with the SiO_2. After curing the graphene/PMMA layer on the MEA on a hotplate at 180 °C for 90 s, organic cleaning of the sample removed the PMMA until only graphene remained in the central region of the MEA.

After the transfer of graphene to the MEA, the circular microelectrodes were defined on the graphene using the same direct writing process with the factory recommended alignment procedure for patterning the electrodes over the graphene/TiN tracks previously deposited. The graphene was then removed from all areas outside of the microelectrodes using oxygen plasma. Therefore, we introduced a modification in the standard oxygen plasma corrosion process applied to silicon substrates. For our glass substrate and for the photoresist thickness employed herein, the optimum plasma corrosion parameters were a power of 300 W, an O_2 flow of 50 sccm, and a pressure of 100 mTorr, for 5 min.

D. Insulation

Next was the formation of the MEA insulation layer. As discussed in Sec. I, the choice of the insulating material is crucial to mitigate parasitic capacitances between the electrodes and the culture medium. Further, the insulation material used here must be fully capacitive and should not reduce the transparency of the MEA achieved by the interlayer.[4,13] Thus, to fulfill these requirements, the material used herein was SU-8 (Microchem, Westborough, USA) with a thickness of 600 nm. The insulation layer was defined and fabricated using the aligned direct write procedure previously described for the conducting area using H-nu 470 photoinitiator for the SU-8 exposure, since our system operates at 405 nm (Sec. II C).[22]

E. Ring

Finally, a glass ring was placed in the center of the MEA device, thereby creating a reservoir for the biological medium at the microelectrode region. The ring allows electrochemical measurements and ensures that the culture medium does not evaporate too quickly during cells experiments, because it contains a sufficient volume of biological material.[13] The glass rings were produced in-house, and the internal and external ring diameters were 2.4 and 2.6 cm, respectively. To maintain the biocompatibility of all materials comprising the MEA, the

ring was affixed to the device using polydimethylsiloxane (Sylgard® 184, Dow Corning, 10:1 ratio).

III. RESULTS AND DISCUSSION

After fabricating the MEAs with 20 and 40 μm diameter graphene microelectrodes, TiN tracks and contact pads, and SU-8 insulation layer on the glass substrate (see Fig. 1).

A. Structural observation

Initial characterization of the MEA confirmed the number and location of the microelectrodes and the absence of short circuits between them. Figure 1 shows a photograph of the entire MEA, and Fig. 2 shows a scanning electron microscope image obtained via FEI Nanolab 200 instrument (Hillsboro, USA) of two microelectrodes in the active region where the electrodes and biological material were concentrated during the experiments.

From Fig. 2, it is possible to observe the arrangement and alignment of the microelectrodes and the presence of graphene at the region. In addition, no broken or short-circuited tracks were observed, signifying that an adequate lithographic process was performed.

B. Electrode characterization

1. Investigation of graphene microelectrodes

To examine the quality of the MEA microelectrodes, first we characterized the graphene using Raman spectroscopy. Raman is an important tool, investigating the material quality, confirming that the transfer was done satisfactorily, and determining the number of graphene layers on the MEA. The equipment used herein was a Raman spectrometer (Renishaw, Wotton-under-edge, England) with a 488 nm excitation wavelength laser, and the response obtained from the graphene on our MEA is shown in Fig. 3.

As can be seen, the graphene in this device exhibited the typical Raman peaks of graphene, exhibiting a peak from the G band at ~1575 cm^{-1} and one Lorentzian profile of the 2D band at ~2690 cm^{-1}. The latter peak is sharp and symmetric with a full width at half maximum close to 100 cm^{-1}, signifying the presence of one or two layers of graphene. We obtained the ratio of the G and 2D peak intensities (I_G/I_{2D}) that are related with graphene doping[23,24] due to the presence of a metal as substrate (TiN). Furthermore, the position of 2D peak is related to the strain in graphene flake when considering contact doping. In addition, considering the low intensity of the D peak at ~1350 cm^{-1}, it is reasonable to infer that a low density of defects and impurities exists in the graphene transferred to the MEA.[16] The 2D band peak at ~1620 cm^{-1} shows a strain at graphene,[25] probably due to the transfer process. Therefore, the Raman spectra results show that the transfer of graphene to the MEA and the lithography and corrosion steps were satisfactory, with an acceptable defect density on the graphene.

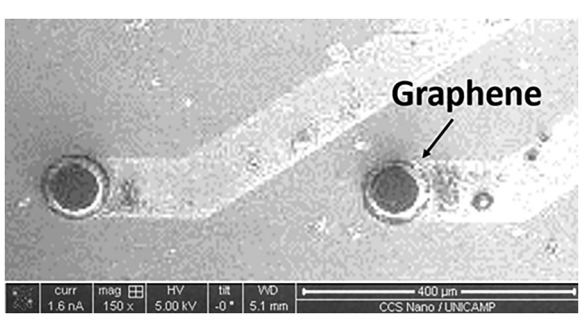

FIG. 2. Scanning electron microscope image of the MEA, showing the arrangement of two graphene covered TiN microelectrodes.

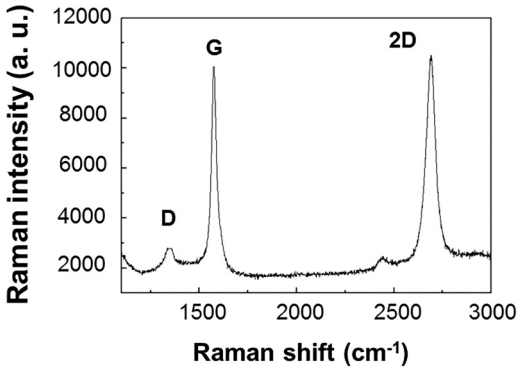

FIG. 3. Raman spectrum from the transferred graphene over TiN microelectrode region of the MEA.

2. Electrochemical characterization of the microelectrodes

Neural activity is captured as an extracellular potential, called the action potential, when an electrode close to the target neuron detects the firing of a single neuron. For this purpose, the signal-to-noise ratio is expected to be approximately 5:1 or greater during a recording of a single neural unit. Although much of the noise typically originates from neural noise (i.e., from an infinite number of undifferentiated action potentials), noise is also influenced by the electrode impedance. Furthermore, the combination of a high electrode impedance (which produces a lower signal-to-noise ratio) and the capacitance between electrode and amplifier system will minimize the response of the former at high frequencies.[14] As a result, three further tests must be performed to characterize the microelectrodes: noise level, cyclic voltammetry (CV) and impedance spectroscopy (IS).

Noise level measurements were obtained by recording the electrical potentials in the fabricated MEA, which identified if the microelectrodes were functioning or if they were defective. For this classification, the results for our MEA were compared to a standard commercially available MEA obtained from MultiChannel Systems (Standard model, Germany).

First, the reservoir created by the ring was filled with 10 mM of phosphate buffered saline (PBS, composed of 0.01M phosphate buffer, 0.0027M potassium chloride, 0.137M sodium chloride, with *p*H equal to 7.4), whereupon the MEA was coupled to the MultiChannel Systems socket and this assembly was then connected to the amplifier, with the MEA reference electrode (the biggest track, see Fig. 1)

connected to the amplifier ground channel. The noise measurement was performed with the MEAs and electrical fixture inside a home-made Faraday cage built with carbon steel sheets with a thickness of 0.5 mm and properly grounded with the potentiostat. Cables from the MEA lead to a potentiostat/ galvanostat PGSTAT12 containing FRA2 electrochemical impedance spectroscopy module (Metrohm-Autolab, Utrecht, Netherlands) amplifier system with a gain of 1000 between the signal at the input of the test microelectrodes and the final output after amplification, and with no digital filtering. The same noise measurement procedure was adopted for the standard commercial MEA device. In this way, because there was no biological culture in the reservoir, it is expected that the detected signals originate only from the thermal noise of the amplifiers. Figure 4 shows the noise amplitude for two sample graphene microelectrodes of two different fabricated MEAs with our process.

As can be seen in Fig. 4, the amplitude of the noise observed from the microelectrodes of the fabricated MEA is generally low, and this result is compatible with that obtained for the standard commercial MEA and is within the expected range.[18] However, it is possible to notice a small difference when comparing the recorded value of devices 1 and 2. This is mainly due to some variation during the process of deposition of the conductor and/or insulation, which ends up affecting this result. An amplitude of about $\pm 5\,\mu$V is noted for the channel for the fabricated MEA, while for the commercial MEA, this level can be up to $\pm 10\,\mu$V and exhibit a random form (data not shown). Consequently, the fabricated graphene microelectrodes exhibited acceptable noise sensitivity, lower than those of commercial MEAs. To confirm this result, we obtained the root mean square (RMS) value of the noise signal.

For the raw signal (i.e., without filtering), the achieved RMS level of the fabricated graphene microelectrodes was $2.46\,\mu$V. This RMS level is well within the range that is considered functional, which goes up to $5\,\mu$V.[19]

We carried out CV measurements to obtain the reduction and oxidation reactions of molecular species in the microelectrodes.[26] In the CV procedure, the potential of a working electrode is varied cyclically and at a constant rate relative to a reference electrode (generally Ag|AgCl) between two levels, while simultaneously allowing current conduction between the working electrode and a counter electrode.[14] Herein, CV testing was applied to detect if the fabricated MEA microelectrodes worked properly and could perform the functions of detecting and/or stimulating cellular electrical signals. The CV test was conducted using 10 mM of PBS in the reservoir, with platinum and Ag|AgCl electrodes as the counter and reference electrodes, respectively, and a single MEA microelectrode as the working electrode. The resulting voltammogram for our graphene MEA microelectrode and for the commercial MEA is given in Fig. 5.

The almost rectangular-shaped waveform of the curve in Fig. 5 shows that the graphene/TiN electrodes have the expected behavior for materials exhibiting only a double-layer capacitance.[14] Further, the CIC value can be determined from the CV curve. The CIC governs the maximum charge that the microelectrode is able to inject without exceeding the water reduction potential window at -0.6 V and can be obtained via the integral along the CV curve divided by the sweep rate.[16] For our fabricated graphene MEA, the mean value of the CIC is 0.7 mC/cm^2, which is a value higher than the amplitudes obtained from MEAs reported in the literature[2,27] and is a satisfactory value. To date, however, no other studies have reported results from MEAs similar to those developed herein,

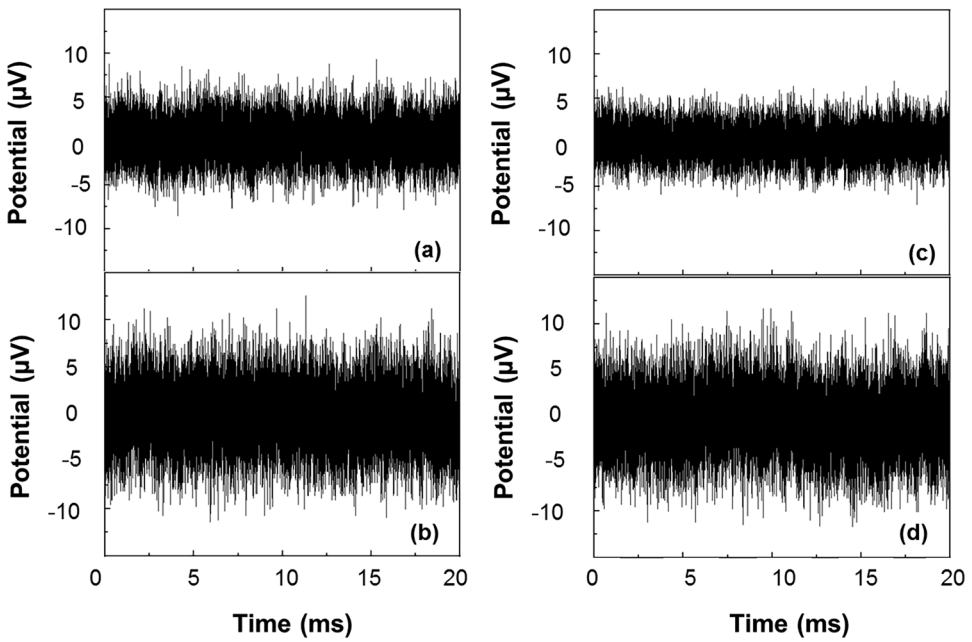

FIG. 4. Noise signal (μV) registered from four graphene microelectrodes of two different fabricated MEAs as a function of time. Curves (a) and (c) consist of the results obtained for the first device and (b) and (d) for the second one. The active area contains PBS, and the recording was performed in all channels simultaneously.

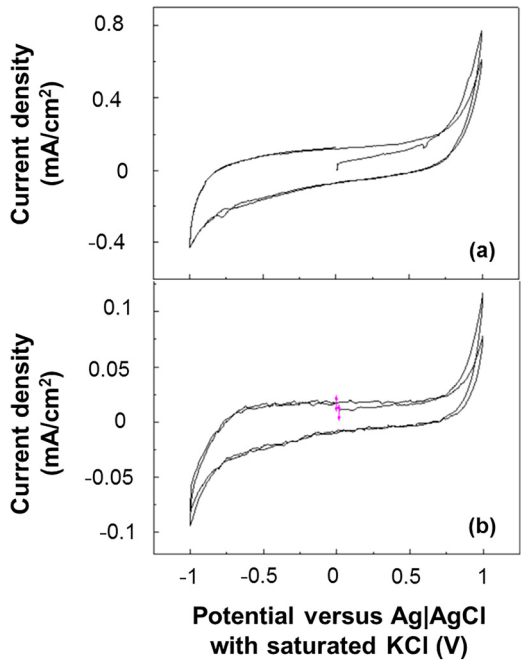

FIG. 5. Cyclic voltammogram for one microelectrode chosen randomly from the (a) fabricated MEA and (b) commercial MEA, both immersed in PBS and scanned at 20 mV s^{-1}.

i.e., composed of graphene microelectrodes with TiN tracks and contact pads. In general, studies found in the literature report larger graphene electrodes compared to those manufactured and discussed in this paper. Comparing the response from our devices to previous studies for graphene electrodes, the result obtained in this work is also interesting. Koerbitzer *et al.*[16] have reported different types of electrodes (0.31 mm^2) and found the CIC values of 0.03, 0.02, and 0.8 mC/cm^2 for pure gold, graphene on gold, and graphene on SiO_2, respectively. It is evident from these results that the addition of graphene on the gold does not significantly improve the electrochemical properties of gold, while the response of graphene on SiO_2 is quite positive and superior to the CIC value found for commercial MEA herein (TiN electrodes) that exhibited a value of 0.11 mC/cm^2.

Impedance spectroscopy is another important test to determine if the microelectrodes work properly and to evaluate the quality of the produced sensor. First, a sinusoidal excitation between ~10 and 50 mV of unit frequency (<1 to 10^5 Hz) is applied to the electrode and the resulting current at each frequency is obtained. With this information, it is possible to find the real and imaginary parts of the electrical impedance and the phase angle. Based on this, the experimental setup for IS measurement herein followed the same protocol adopted for the CV testing. Figure 6 shows the acquired impedance and phase modulus curves as a function of frequency from 1 Hz to 10 kHz for one microelectrode chosen randomly in the fabricated MEA. It can be seen in Fig. 6 that both impedance and phase are frequency dependent. Unlike other materials, however, the impedance of the graphene microelectrode is variable, depending on the state of the material, its manufacturing process, its surface area, and whether or not it is employed with doping.[17]

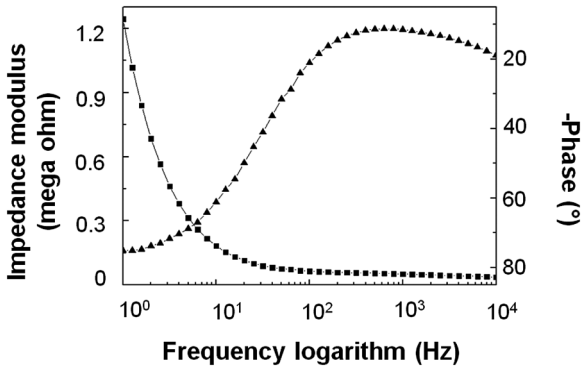

FIG. 6. Impedance modulus (rectangular symbol, left axis) and phase (triangular symbol, right axis) as a function of the logarithm of the frequency for one microelectrode chosen randomly in the fabricated MEA.

Highly relevant information regarding the MEA performance that can be extracted from the IS curve is the impedance modulus at 1 kHz,[15,16] which is directly related to the noise that appears on the electrodes. It has been suggested that the microelectrodes must exhibit the lowest impedance possible for optimal experimental recording.[6] Thus, if the value of the impedance modulus at 1 kHz is between 1 kΩ and 1 MΩ and decreasing with increasing frequency and if the phase is around 80°, the MEA performance is considered adequate.[4,14] The fabricated MEA herein exhibited an average impedance at 1 kHz of ~5.2 kΩ, which is satisfactory and lower than those reported in the literature.[28,29] Du *et al.*[17] have reported the impedance of MEAs with graphene and with gold electrodes (diameter of 20 μm) tested at frequencies between 0.1 and 100 kHz, where the impedance levels of the graphene electrode (170 kΩ) were relatively lower than that of the gold electrode (186 kΩ). Further, Koerbitzer *et al.*[16] have compared the impedance of three types of electrodes (gold, graphene/SiO_2, and graphene/gold; 0.31 mm^2 area) at frequencies between 1 Hz and 1 MHz, where the impedance level value of graphene/gold electrode was the lowest (4.4 kΩ), though those of gold (7 kΩ) and graphene/SiO_2 (10 kΩ) were relatively close. Herein, the impedance level of the fabricated MEA device was also compatible with that of the commercial MEA, whose impedance was in the range of 30–400 kΩ.[7]

IV. SUMMARY AND CONCLUSIONS

We confirm that a graphene-based MEA was successfully manufactured with the process developed herein, from the choice of the substrate to the definition of graphene patterns, and the fabricated MEA generated interesting responses. The charge injection capacity of the fabricated microelectrodes was four times greater than those found for the commercially available MEA from MultiChannel Systems, where the latter possessed TiN electrodes of comparable dimension to those herein. Further, the use of graphene in the microelectrode region rendered it completely transparent and thus facilitated the experimental observation of the biological environment. Thus, graphene was shown to be a good alternative to

replace traditional conductors as MEA microelectrodes, since it is known to be biocompatible and exhibit low noise and high electrical conductivity and good long-term stability in aqueous solutions.[2,17] Therefore, we have successfully fabricated a new type of MEA whose microelectrode response is within a suitable range that is comparable with commercial MEAs. Consequently, our device is adequate to measure cellular potentials.

ACKNOWLEDGMENTS

This work was performed in part at the Center of Semiconductor Components and Nanotechnologies (CCSNano), a member of SisNano (CNPq process 402299/2013-2), and part at the Center of Information Technology Renato Archer (CTI). Thus, the authors would like to acknowledge the financial support from Coordenação de Aperfeiçoamento de Pessoal de Nível Superior (CAPES) Brazilian Foundation and from INCT/CNPq-NAMITEC. They would also like to thank Dunieskys R.G. Larrude from the Mackgraphe Center at Mackenzie University, São Paulo, Brazil FAPESP Project No. 14/24944-0 for the graphene on Cu deposition. The authors are also grateful to the "Gleb Wataghin" Institute of Physics, at the State University of Campinas, for the manufacture of the glass rings.

[1]Y. H. Kim, N. S. Baek, Y. H. Han, A.-Y. Kim, M.-A. Chung, and S.-D. Jung, J. Micromech. Microeng. **23**, 97001 (2013).
[2]D. Kuzum *et al.*, Nat. Commun. **5**, 5259 (2014).
[3]W. Lee, D. Kim, N. Matsuhisa, M. Nagase, M. Sekino, G. G. Malliaras, T. Yokota, and T. Someya, Proc. Natl. Acad. Sci. U.S.A. **114**, 10554 (2017).
[4]M. Taketani and M. Baudry, *Advances in Network Electrophysiology: Using Multi-electrode Arrays*, 1st ed. (Springer, New York, 2006), pp. 24–35.
[5]Z. Aqrawe, J. Montgomery, J. Travas-Sejdic, and D. Svirskis, Trends Biotechnol. **35**, 93 (2017).
[6]R. Kim, S. Joo, H. Jung, N. Hong, and Y. Y. Nam, Biomed. Eng. Lett. **4**, 129 (2014).
[7]M. Systems, *Microelectrode Array (MEA) Manual* (MultiChannel Systems MCS GmbH, Reutlingen, Germany, 2017), pp. 1–68.
[8]N. J. Killian, V. N. Vernekar, S. M. Potter, and J. Vukasinovic, Front. Neurosci. **10**, 135 (2016).
[9]V. Pasquele, P. Massobrio, L. L. Bologna, M. Chiappalone, and S. Martinoia, Neuroscience **153**, 1354 (2008).
[10]A. Bhatti, K. H. Lee, H. Garmestani, and C. P. Lim, *Emerging Trends in Neuroengineering and Neural Computation*, 1st ed. (Springer, Singapore, 2017), pp. 3–59.
[11]K. Harris, Curr. Protoc. Pharmacol. **71**, 11.18.1 (2015).
[12]Y. H. Tennico, M. T. Koesdjojo, S. Kondo, D. T. Manrell, and V. T. Remcho, Sens. Actuators B **143**, 799 (2010).
[13]K. Wang, H. A. Fishman, H. Dai, and J. S. Harris, Nanoletters **6**, 2043 (2006).
[14]S. F. Cogan, Annu. Ver. Biomed. Eng. **10**, 275 (2008).
[15]D.-W. Park *et al.*, Nat. Commun. **5**, 5258 (2014).
[16]B. Koerbitzer, P. Krauss, C. Nick, S. Yadav, J. J. Schneider, and C. Thielemann, 2D Mater. **3**, 024004 (2016).
[17]Y. Du, L. Wu, J. Cheng, S. Huang, Q. Cai, Q. Jin, and J. Zhao, J. Biol. Phys. **41**, 339 (2015).
[18]V. P. Gomes, A. D. Barros, J.-N. Destro-Filho, S. Martinoia, A. Pasquarelli, and J. W. Swart, J. Integr. Circ. Syst. **11**, 1 (2016).
[19]D. G. Larrude, T. Garcia-Basabe, F. L. F. Junior, and M. L. M. Rocco, Royal Soc. Chem. Adv. **5**, 74189 (2015).
[20]L. Jiao, B. Fan, X. Xian, Z. Wu, J. Zhang, and Z. Liu, J. Am. Chem. Soc. **130**, 12612 (2008).
[21]X. S. Li, Y. W. Zhu, W. W. Cai, M. Borysiak, B. Y. Han, D. Chen, R. D. Piner, L. Colombo, and R. S. Ruoff, Nano Lett. **9**, 4359 (2009).
[22]J. C. Ramirez, J. N. Schianti, M. G. Almeida, A. Pavani, R. R. Panepucci, H. E. Hernandez-Figueroa, and L. H. Gabrielli, Opt. Mat. Express **7**, 2651 (2017).
[23]R. Beams, L. G. Cançado, and L. Novotny, J. Phys. Condens. Matter. **27**, 083002 (2015).
[24]A. Das *et al.*, Nat. Nanotechnol. **3**, 210 (2008).
[25]A. C. Ferrari *et al.*, Phys. Rev. Lett. **97**, 187401 (2006).
[26]N. Elgrishi, K. J. Rountree, B. D. McCarthy, E. S. Rountree, T. T. Eisenhart, and J. L. Dempsey, J. Chem. Educ. **95**, 197 (2017).
[27]A. M. H. Ng, Y. Wang, W. C. Lee, L. C. Teck, K. P. Loh, and H. Y. Low, Carbon. **67**, 390 (2014).
[28]C. W. Jeong, G. H. Kim, N. Y. Kim, Z. Lee, S. D. Jung, and J.-O. Lee, Roy. Soc. Chem. Adv. **7**, 3273 (2017).
[29]D.-W. Park *et al.*, Nat. Commun. **5**, 5258 (2014).